We are IntechOpen, the world's leading publisher of Open Access books Built by scientists, for scientists

4,800
Open access books available

122,000
International authors and editors

135M
Downloads

Our authors are among the

154
Countries delivered to

TOP 1%
most cited scientists

12.2%
Contributors from top 500 universities

CLARIVATE ANALYTICS BOOK CITATION INDEX INDEXED

WEB OF SCIENCE™

Selection of our books indexed in the Book Citation Index in Web of Science™ Core Collection (BKCI)

Interested in publishing with us?
Contact book.department@intechopen.com

Numbers displayed above are based on latest data collected.
For more information visit www.intechopen.com

28

Dynamic Modelling and Motion Control for Underwater Vehicles with Fins

Xiao Liang, Yongjie Pang, Lei Wan and Bo Wang
Harbin Engineering University
China

1. Introduction

With the development of the activities in deep sea, the application of the autonomous underwater vehicle (AUV) is very widespread and there is a prominent prospect. The development of an AUV includes many areas, such as vehicle (carrier/platform) design, architecture, motion control, intelligent planning and decision making, etc (Blidberg 1991; Xu et al., 2006). The researchers dedicate themselves to improving the performance of modular, low-cost AUVs in such applications as long-range oceanographic survey, autonomous docking, and shallow-water mine countermeasures. These goals can be achieved through the improvement of maneuvering precision and motion control capability with energy constraints. For low energy consumption, low resistance, and excellent maneuverability, fins are usually utilized to modify the AUV hydrodynamic force. An AUV with fins can do gyratory motion by vertical fins and do diving and rising motion by horizontal fins. Therefore, the control system of the propeller-fin-drived AUV is very different to the conventional only-propeller-drived AUV.

A dynamic mathematic model for the AUV with fins based on a combination of theory and empirical data would provide an efficient platform for control system development, and an alternative to the typical trial-and-error method of control system tuning. Although some modeling and simulation methods have been proposed and applied (Conte et al., 1996; Timothy, 2001; Chang et al., 2002; Ridley, 2003; Li et al., 2005; Nahon, 2006; Silva et al., 2007), there is no standard procedure for modeling AUVs with fins in industry. Therefore, the simulation of the AUVs with fins is a challenge.

This chapter describes the development and verification of a six Degree of Freedom (DOF), non-linear model for an AUV with fins. In the model, the external force and moment resulting from hydrostatics, hydrodynamic lift and drag, added mass, and the thrusters and fins are all analyzed and expressed in matrix form. The equations describing the rigid-body dynamics are left in non-linear form to better simulate the AUV inherently non-linear behavior. Motion simulation is achieved through numeric integration of the motion equations. The simulation output is then checked with the AUV dynamics data collected in experiments at sea. The comparison results show that the non-linear model gives an accurate estimation of the AUV's acutal motion. The research objective of this project is the development of WEILONG mini-AUV, which is a small, low-cost platform serving in a range of oceanographic applications (Su et al., 2007).

Source: Underwater Vehicles, Book edited by: Alexander V. Inzartsev,
ISBN 978-953-7619-49-7, pp. 582, December 2008, I-Tech, Vienna, Austria

Due to the effect of fins, conventional control methods can not meet the requirement for motion control (Giusepp, 1999). It requires high response speed and robustness to improve the maneuverability, at the same time the controller's compute process should be simple enough. This chapter proposes a new control method which is adaptive to the AUV with fins—S surface control (Liu et al., 2001). S surface controller is developed from sigmoid function and the idea of fuzzy control which has been proved efficient in ocean experiments. It has a simple structure requiring only two inputs, but it is applicable to nonlinear system. Moreover, we will deduce self-learning algorithm using BP algorithm of neural networks for reference (Liu et al., 2002). Finally, experiments are conducted on WEILONG AUV to verify the feasibility and superiority.

2. Mathematic modelling of AUV motion

2.1 Coordinate system and motion parameters definition

In order to describe the AUV motion and set up a 6-DOF nonlinear mathematical model, a special reference frames have been established (Shi, 1995). There are two reference frames: fixed reference frame *E-ξηζ* (or inertial coordinate system) and motion reference frame *o-xyz* (or body-fixed coordinate system), which are shown in Fig.1.

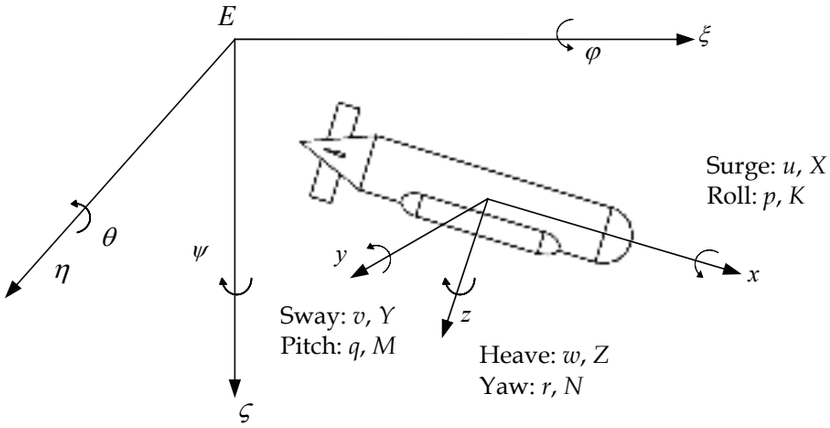

Fig. 1. Body-fixed and inertial coordinate system

Considering the shape characteristic of most AUVs, the mathematic model is based on the hypothesis that the AUV is symmetric about its *xoz* plane.

Defining generalized position vector $\mathbf{R}$, generalized velocity vector $\mathbf{V}$ and generalized force vector $\boldsymbol{\tau}$, the motion vector include

1. Position and attitude (in *E-ξηζ*)

$$\mathbf{R} = [\mathbf{r}^T, \boldsymbol{\Lambda}^T]^T, \mathbf{r} = [\xi, \eta, \zeta]^T, \boldsymbol{\Lambda} = [\varphi, \theta, \psi]^T$$

2. Linear and angular velocities (in *o-xyz*)

$$\mathbf{V} = [\mathbf{U}^T, \boldsymbol{\Omega}^T]^T, \mathbf{U} = [u, v, w]^T, \boldsymbol{\Omega} = [p, q, r]^T$$

3. Force and moment parameters (in *o-xyz*)

$$\boldsymbol{\tau} = [\mathbf{F}^T, \mathbf{M}^T]^T, \mathbf{F} = [X, Y, Z]^T, \mathbf{M} = [K, M, N]^T$$

2.2 Dynamics model

Based on momentum theorem, the AUV dynamic equation is

$$\mathbf{M}_{RB}\dot{\mathbf{V}} + \mathbf{C}_{RB}(\mathbf{V})\mathbf{V} = \boldsymbol{\tau} \tag{1}$$

where $\mathbf{M}_{RB}$ is the generalized mass matrix of the AUV body, and $\mathbf{C}_{RB}(\mathbf{V})$ is the Coriolis and centripetal force matrix. $\mathbf{M}_{RB}$ is given by

$$\mathbf{M}_{RB} = \begin{bmatrix} m & 0 & 0 & 0 & mz_G & -my_G \\ 0 & m & 0 & -mz_G & 0 & mx_G \\ 0 & 0 & m & my_G & -mx_G & 0 \\ 0 & -mz_G & my_G & J_x & J_{xy} & J_{xz} \\ mz_G & 0 & -mx_G & J_{yx} & J_y & J_{yz} \\ -my_G & mx_G & 0 & J_{zx} & J_{zy} & J_z \end{bmatrix} \tag{2}$$

where m is the AUV mass, J terms represent the inertial tensors, and x_G, y_G, z_G represent the AUV position barycenter in body-fixed frame. $\mathbf{C}_{RB}(\mathbf{V})$ is given by

$$\mathbf{C}_{RB}(\mathbf{V}) = \begin{bmatrix} 0 & -mr & mq \\ mr & 0 & -mp \\ -mq & mp & 0 \\ -m(y_Gq + z_Gr) & my_Gp & mz_Gp \\ mx_Gu & -m(z_Gr + x_Gp) & mz_Gq \\ mx_Gr & my_Gr & -m(x_Gp + y_Gq) \end{bmatrix}$$
$$\begin{bmatrix} m(y_Gq + z_Gr) & -mx_Gq & -mx_Gr \\ -my_Gp & m(z_Gr + x_Gp) & -my_Gr \\ -mz_Gp & -mz_Gq & m(x_Gp + y_Gq) \\ 0 & J_{zx}p + J_{zy}q + J_zr & -J_{yx}p - J_yq - J_{yz}r \\ -J_{zx}p - J_{zy}q - J_zr & 0 & J_xp + J_{xy}q + J_{xz}r \\ J_{yx}p + J_yq + J_{yz}r & -J_xp - J_{xy}q - J_{xz}r & 0 \end{bmatrix} \tag{3}$$

Generalized force vector $\boldsymbol{\tau}$ at the right of the equation (1) is outside force (or moment) acting on the AUV, including static force vector $\boldsymbol{\tau}_G$ (gravity and buoyancy), hydrodynamics force vector of the vehicle body (include $\boldsymbol{\tau}_A$ which is caused by added mass and viscous damping force $\boldsymbol{\tau}_V$), and the controlled forece vector (include the thruster force $\boldsymbol{\tau}_{prop}$ and the fin force $\boldsymbol{\tau}_R$). The static force vector $\boldsymbol{\tau}_G$ reflects the effect of the vehicle weight and buoyancy. The vehicle's weight is $W = mg$ and the buoyancy is $B = \rho\nabla g$, where ρ is the dentisity of the surrounding fluid, and ∇ is the total volume displaced by the AUV. Therefore, $\boldsymbol{\tau}_G$ is given by

$$\boldsymbol{\tau}_G = \begin{bmatrix} X_G \\ Y_G \\ Z_G \\ K_G \\ M_G \\ N_G \end{bmatrix} = \begin{bmatrix} -(W - B)\cdot\sin\theta \\ (W - B)\cdot\sin\varphi\cos\theta \\ (W - B)\cdot\cos\varphi\cos\theta \\ (y_GW - y_BB)\cdot\cos\varphi\cos\theta - (z_GW - z_BB)\cdot\sin\varphi\cos\theta \\ -(x_GW - x_BB)\cdot\cos\varphi\cos\theta - (z_GW - z_BB)\cdot\sin\theta \\ (x_GW - x_BB)\cdot\sin\varphi\cos\theta - (y_GW - y_BB)\cdot\sin\theta \end{bmatrix} \tag{4}$$

where x_B, y_B, z_B are the vehicle coordinates in body-fixed coordinate system.
$\boldsymbol{\tau}_{\mathbf{A}}$ which is related with added mass is given by

$$\boldsymbol{\tau}_A = -(\mathbf{M}_A\dot{\mathbf{V}} + \mathbf{C}_A(\mathbf{V})\mathbf{V}) \tag{5}$$

where $\mathbf{M}_A$ is the added mass matrix given by

$$\mathbf{M}_A = \begin{bmatrix} \lambda_{11} & 0 & \lambda_{13} & 0 & \lambda_{15} & 0 \\ 0 & \lambda_{22} & 0 & \lambda_{24} & 0 & \lambda_{26} \\ \lambda_{31} & 0 & \lambda_{33} & 0 & \lambda_{35} & 0 \\ 0 & \lambda_{42} & 0 & \lambda_{44} & 0 & \lambda_{46} \\ \lambda_{51} & 0 & \lambda_{53} & 0 & \lambda_{55} & 0 \\ 0 & \lambda_{62} & 0 & \lambda_{64} & 0 & \lambda_{66} \end{bmatrix} \tag{6}$$

where λ terms are the vehicle added mass.
$\mathbf{M}_A$ can be also denoted as hydrodynamic coefficients expression as follows:

$$\mathbf{M}_A = -\begin{bmatrix} X_{\dot{u}} & 0 & X_{\dot{w}} & 0 & X_{\dot{q}} & 0 \\ 0 & Y_{\dot{v}} & 0 & Y_{\dot{p}} & 0 & Y_{\dot{r}} \\ Z_{\dot{u}} & 0 & Z_{\dot{w}} & 0 & Z_{\dot{q}} & 0 \\ 0 & K_{\dot{v}} & 0 & K_{\dot{p}} & 0 & K_{\dot{r}} \\ M_{\dot{u}} & 0 & M_{\dot{w}} & 0 & M_{\dot{q}} & 0 \\ 0 & N_{\dot{v}} & 0 & N_{\dot{p}} & 0 & N_{\dot{r}} \end{bmatrix} \tag{7}$$

$\mathbf{C}_A(\mathbf{V})$ is a Coriolis-like matrix induced by $\mathbf{M}_A$,

$$\mathbf{C}_A(\mathbf{V}) = \begin{bmatrix} 0 & 0 & 0 & 0 & a_3 & -a_2 \\ 0 & 0 & 0 & -a_3 & 0 & a_1 \\ 0 & 0 & 0 & a_2 & -a_1 & 0 \\ 0 & a_3 & -a_2 & 0 & b_3 & -b_2 \\ -a_3 & 0 & a_1 & -b_3 & 0 & b_1 \\ a_2 & -a_1 & 0 & b_2 & -b_1 & 0 \end{bmatrix} \tag{8}$$

where

$$a_1 = \lambda_{11}u + \lambda_{13}w + \lambda_{15}q \qquad a_2 = \lambda_{22}v + \lambda_{24}p + \lambda_{26}r \qquad a_3 = \lambda_{31}u + \lambda_{33}w + \lambda_{35}q$$

$$b_1 = \lambda_{42}v + \lambda_{44}p + \lambda_{46}r \qquad b_2 = \lambda_{51}u + \lambda_{53}w + \lambda_{55}q \qquad b_3 = \lambda_{62}v + \lambda_{64}p + \lambda_{66}r$$

The viscous damping force $\boldsymbol{\tau}_V$ is given by

$$\boldsymbol{\tau}_V = \mathbf{D}(\mathbf{V})\mathbf{V} \tag{9}$$

The damping matrix $\mathbf{D}(\mathbf{V})$ is given by

$$\mathbf{D}(\mathbf{V}) = \begin{bmatrix} X_u + X_{u|u|}|u| & 0 & 0 & 0 & 0 & 0 \\ 0 & Y_v + Y_{v|v|}|v| & 0 & 0 & 0 & 0 \\ Z_0|u| & 0 & Z_w + Z_{w|w|}|w| & 0 & 0 & 0 \\ 0 & 0 & 0 & K_p + K_{p|p|}|p| & 0 & 0 \\ M_0|u| & 0 & 0 & 0 & M_q + M_{q|q|}|q| & 0 \\ 0 & 0 & 0 & 0 & 0 & N_r + N_{r|r|}|r| \end{bmatrix} \quad (10)$$

where X_u, Y_v, Z_w, K_p, M_q, and N_r are the linear damping coefficients. $Y_{v|v|}$, $Z_{w|w|}$, $K_{p|p|}$, $M_{q|q|}$, $X_{u|u|}$, and $N_{r|r|}$ are the quadratic damping coefficients. M_0 and Z_0 are the effect caused by the dissymmetry on *xoy* plane.

The external force and moment vector produced by trusters $\boldsymbol{\tau}_{prop}$ is defined as

$$\boldsymbol{\tau}_{prop} = \mathbf{L}\mathbf{T}_{prop} \quad (11)$$

where $\mathbf{L}$ is a mapping matrix, and $\mathbf{T}_{prop}$ is the thrust vector produced by thrusters given by

$$\mathbf{T}_{prop} = \begin{bmatrix} T_1 \\ T_2 \\ \vdots \\ T_n \end{bmatrix} \quad (12)$$

The number n in $\mathbf{T}_{prop}$ depends on the number of thrusters. The mapping matrix $\mathbf{L}$ is a 6×n matrix that uses $\mathbf{T}_{prop}$ to find the overall force and moment acting on the vehicle.

Hydrodynamics of a single thruster is usually obtained through the in water test. A series of advance coefficient J corresponding to the thrust coefficient K_T data can be obtained from the in water test. Data from an in water test are shown in Fig.2. We fit the curve by the method of least squares and then obtain the fitted $J - K_T$ curve. In practical appilcations, we get advance coefficient J and substitute it into fitted $J - K_T$ curve to obtain K_T. Finally, the thrust can be obtained. Detailed process is as follows:

1. We get the advance coefficient J from fluid velocity cross the propeller V_{prop}, the propeller diameter D, and the screw propeller rotate speed n (n is determined by controller): $J = \dfrac{V_{prop}}{nD}$.
2. We put J into fitted $J - K_T$ curve to get force coefficient K_T.
3. We get thrust- $\mathbf{T}$ by using equation $\mathbf{T} = K_T n^2 D^4$.

The overall external force and moment vector produced by fins $\boldsymbol{\tau}_R$ is given by

$$\boldsymbol{\tau}_R = \begin{bmatrix} X_R \\ Y_R \\ Z_R \\ K_R \\ M_R \\ N_R \end{bmatrix} \quad (13)$$

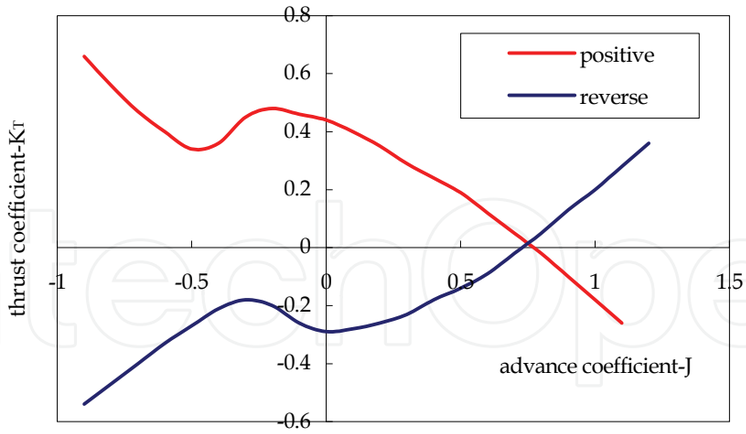

Fig. 2. Capability curves of thrusters

According to every single fin force and its installating position, $\boldsymbol{\tau}_R$ can be obtained.
As to a control fin on the vehicle, the hydrodynamic force can be decomposed into two directions: lift force **L**—vertical to stream current and drag force **D**—along stream current. Lift force and drag force can be calculated by the equations as follows:

$$\begin{aligned} \mathbf{L} &= \frac{1}{2} C_L \rho A_R v_e^2 \\ \mathbf{D} &= \frac{1}{2} C_D \rho A_R v_e^2 \end{aligned} \tag{14}$$

where C_L is the fin lift coefficient, C_D is the fin drag coefficient, A_R is the fin planform area, and v_e is the effective fin velocity. The values of lift coefficient C_L and drag coefficient C_D are related with effective fin angle of attack a.

We can adopt experiment, theroy computation, or empirical fomular to get C_L and C_D. Experiment and empirical fomular method will be introduced below.

1. Actual measurement from exprement

A series of data of angles of attack a vs. lift coefficient C_L and drag coefficient C_D can be obtained from hydrodynamic experiment, and then fitted curves of C_L and C_D can be generated through least squares fit. For example, the fitted currves of a fin is shown in Fig.3. When we know the current angle of attack of fin on the AUV, the values of C_L and C_D under this angle can be obtained by curves interpolation.

2. Method of empirical equation

The empirical equations to calculate C_L and C_D are given by

$$C_L = \frac{\partial C_L}{\partial \alpha} \times \alpha + \frac{C_{DC}}{\lambda} \left(\frac{\alpha}{57.3}\right)^2 \tag{15}$$

$$\frac{\partial C_L}{\partial \alpha} = \frac{0.9(2\pi)\lambda}{57.3\left[\cos\Lambda \sqrt{\frac{\lambda^2}{\cos^4\Lambda}} + 4 + 1.8\right]} \tag{16}$$

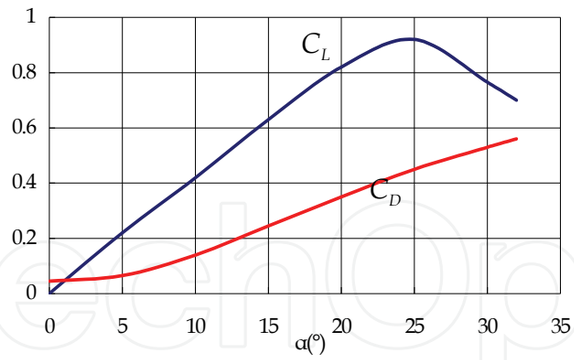

Fig. 3. Lift and drag coefficient curves

$$C_D = C_{d0} + \frac{C_L^{\,2}}{e\pi\lambda} \tag{17}$$

where $\frac{\partial C_L}{\partial \alpha}$ is the slope at a=0 in lift coefficient curves, and C_{DC} is the drag coefficient of cross current which depends on tip shape and rake ratio (e.g. Quadrate tip: C_{DC} =0.8. Smooth tip: C_{DC} =0.4). C_{d0} is the airfoil profile drag coefficient (viscous drag). For the profile section NACA0015, C_{d0} =0.0065. Λ is the sweptback angle at 1/4 chord of the fin. λ is the aspect ratio. a is the angle of attack (degree).

In order to get C_L and C_D, we should know the real effective angle of atttack. As the fin located at some offset from the origin of the AUV coordinate system, it experiences the following effective velocities

$$\begin{aligned} u_{fin} &= u + z_{fin} - y_{fin} r \\ v_{fin} &= v + x_{fin} r - z_{fin} p \\ w_{fin} &= w + y_{fin} - x_{fin} q \end{aligned} \tag{18}$$

where x_{fin}, y_{fin}, and z_{fin} are the body-fixed coordinates of the fin posts.

The effective fin angles of attack δ_{se} and δ_{re} are given by

$$\begin{aligned} \delta_{se} &= \delta_s + \beta_{se} \\ \delta_{re} &= \delta_r + \beta_{re} \end{aligned} \tag{19}$$

where δ_r and δ_s are the fin angles referenced to the vehicle hull, β_{re} and β_{se} are the effective angles of attack of the fin zero plane, as shown in Fig.4. β_{re} and β_{se} are given by

$$\beta_{re} = \frac{v_{fin}}{u_{fin}} = \frac{v + x_{fin} r - z_{fin} p}{u + z_{fin} - y_{fin} r} \qquad \beta_{se} = \frac{w_{fin}}{u_{fin}} = \frac{w + y_{fin} - x_{fin} q}{u + z_{fin} - y_{fin} r} \tag{20}$$

Based on the above analysis, equation (1) could be rewritten into more detailed form

$$(\mathbf{M}_{RB} + \mathbf{M}_A)\dot{\mathbf{V}} = \boldsymbol{\tau}_G + \boldsymbol{\tau}_{prop} + \boldsymbol{\tau}_R + \mathbf{D}(\mathbf{V})\mathbf{V} - (\mathbf{C}_{RB}(\mathbf{V}) + \mathbf{C}_A(\mathbf{V}))\mathbf{V} \tag{21}$$

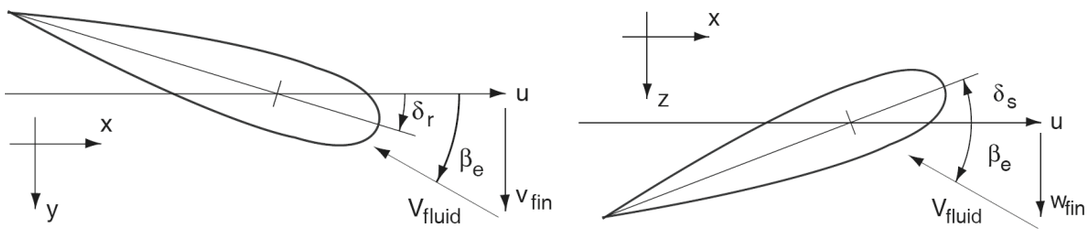

(a) Effective rudder angle of attack (b) Effective stern plane angle of attack

Fig. 4. Effective angle of attack scheme

2.3 Kinematics model

The coordinate transformation between body-fixed coordinate system and inertial coordinate system can is given by

$$\begin{bmatrix} \dot{\xi}_G \\ \dot{\eta}_G \\ \dot{\zeta}_G \\ \dot{\varphi} \\ \dot{\theta} \\ \dot{\psi} \end{bmatrix} = \begin{bmatrix} T_1 & 0_{3\times3} \\ 0_{3\times3} & T_2 \end{bmatrix} \begin{bmatrix} u \\ v \\ w \\ p \\ q \\ r \end{bmatrix} \tag{22}$$

where ξ_G, η_G and ζ_G are the barycentre coordinates in inertial coordinate system, T_1 and T_2 are coordinate transform matrix given by

$$\boldsymbol{T}_1 = \begin{bmatrix} \cos\psi\cos\theta & \cos\psi\sin\theta\sin\varphi - \sin\psi\cos\varphi & \cos\psi\sin\theta\cos\varphi + \sin\psi\sin\varphi \\ \sin\psi\cos\theta & \sin\psi\sin\theta\sin\varphi + \cos\psi\cos\varphi & \sin\psi\sin\theta\cos\varphi - \cos\psi\sin\varphi \\ -\sin\theta & \cos\theta\sin\varphi & \cos\theta\cos\varphi \end{bmatrix} \tag{23}$$

$$\boldsymbol{T}_2 = \begin{bmatrix} 1 & \tan\theta\sin\varphi & \tan\theta\cos\varphi \\ 0 & \cos\varphi & -\sin\varphi \\ 0 & \sin\varphi\sec\theta & \cos\varphi\sec\theta \end{bmatrix} \tag{24}$$

2.4 Numerical integration

Given the complex and highly nonlinear nature of the equations (21) and (22), we will use numerical integration to solve these equations and get the vehicle speed, position, and attitude vs time.

The non-linear state equation of the AUV is given by

$$\dot{\mathbf{x}}_n = \mathrm{f}(\mathbf{x}_n, \mathbf{u}_n) \tag{25}$$

where $\mathbf{x}_n$ is the state vector, and $\mathbf{u}_n$ is the input vector:

$$\mathbf{x}_n = [u \quad v \quad w \quad p \quad q \quad r \quad \xi \quad \eta \quad \zeta \quad \varphi \quad \theta \quad \psi]^T \tag{26}$$

$$\mathbf{u}_n = [\boldsymbol{\tau}_{prop} \quad \boldsymbol{\tau}_R] \tag{27}$$

Here, Runge-Kutta method of numerical integration is usually used to solve the equations. Firstly, we calculate the following equations

$$\begin{aligned} k_1 &= \boldsymbol{x}_n + \mathrm{f}(\mathbf{x}_n, \mathbf{u}_n) \\ k_2 &= \mathrm{f}(\mathbf{x} + \frac{\Delta t}{2} k_1, \mathbf{u}_{n+\frac{1}{2}}) \\ k_3 &= \mathrm{f}(\mathbf{x} + \frac{\Delta t}{2} k_2, \mathbf{u}_{n+\frac{1}{2}}) \\ k_4 &= \mathrm{f}(\mathbf{x} + \Delta t k_4, \mathbf{u}_{n+1}) \end{aligned} \tag{28}$$

where the interpolated input vector is

$$\mathbf{u}_{n+\frac{1}{2}} = \frac{1}{2}(\mathbf{u}_n + \mathbf{u}_{n+1}) \tag{29}$$

Then, we combine the above equations

$$\mathbf{x}_{n+1} = \mathbf{x}_n + \frac{\Delta t}{6}(k_1 + 2k_2 + 2k_3 + k_4) \tag{30}$$

2.5 Simulation results

Base on the above mathematic modelling and analysis, many simulation data are obtained using the simulator of one AUV. The simulation results are compared with the results of at-sea experiments. The zigzag-like motions in horizontal plane and vertical plane were simulated and the compared results are shown in Fig.5 and Fig.6.

From the comparison between simulation results and experiment results, we can conclude that the mathematic model of the AUV motion and the numerical integration method are accurate and feasible.

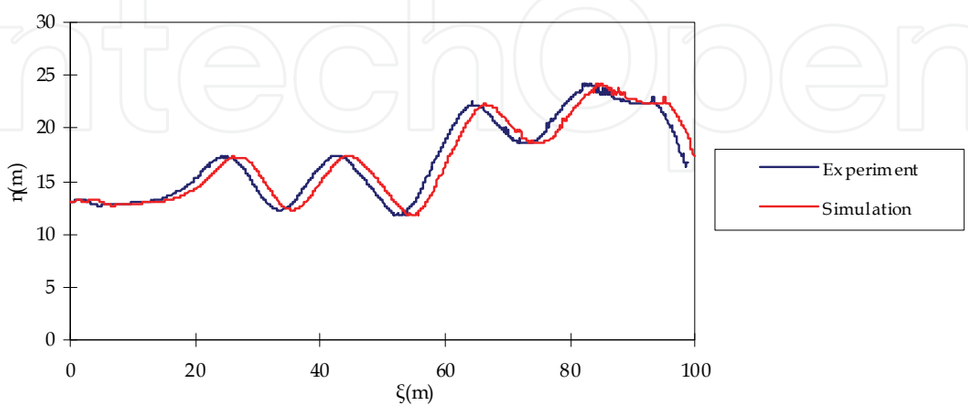

Fig. 5. Zigzag-like motion in horizontal plane

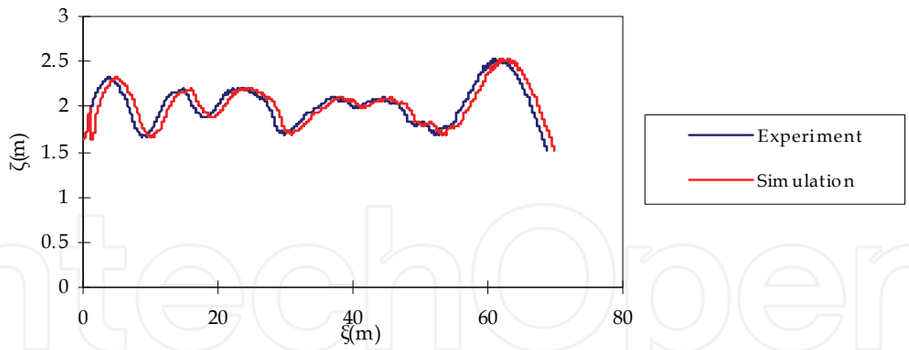

Fig. 6. Zigzag-like motion in vertical plane

2.6 Summary

The nonlinear mathematic model of the AUV motion is constructed in this section and the numerical integration to solve this model is also discussed. Moreover, the model is applicable to most AUVs.

3. AUV motion control

3.1 S surface control

The control rules (Table 1) of the general fuzzy controller indicate that changes of the control outputs are regular. Based on the figures along the leading diagonal, there is a polygonal line, which can be fitted with a smooth curve (a sigmoid function). In fact, the smooth curve can be viewed as innumerable polygonal lines with a length approaching to zero joined together. When designing fuzzy controller, the form (when the deviation is comparatively large, the control demand would be loosely considered; on the contrary, when the deviation is comparatively small, the control demand would be strictly treated) that is loosen at both sides and thick at the middle is generally adopted, which is consistent with the variation form of the sigmoid function. Thus, the sigmoid function incarnates the idea of fuzzy control on a certain extent. Moreover, the fold line surface that corresponds with the whole fuzzy rule of fuzzy control can be replaced with the curved surface composed by smooth curves, as shown in figure 7.

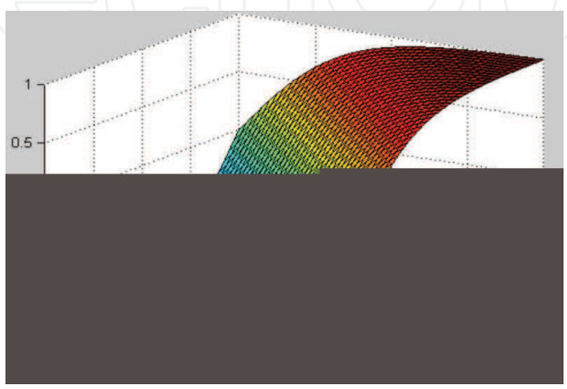

Fig. 7. Sigmoid curved surface

4	3	2	1
3	2	1	0
2	1	0	-2
1	0	-1	-2
0	-1	-2	-3

Table 1. Control rules table

Generally, the function of sigmoid curve is given by

$$y = 2.0/\left(1.0 + e^{-kx}\right) - 1.0 \tag{31}$$

Then, the function of sigmoid curved surface is

$$z = 2.0/\left(1.0 + e^{(-k_1 x - k_2 y)}\right) - 1.0 \tag{32}$$

Thus, the designed control model of S surface controller is

$$u = 2.0/\left(1.0 + e^{(-k_1 e - k_2 \dot{e})}\right) - 1.0 \tag{33}$$

where e and $\dot{e}$ stand for the input information (error and the rate of error change, which are normalized), u is the control output which is the output force (normalized) in each freedom, and k_1 and k_2 are the control parameters corresponding to error and rate of error change respectively.

In equation (33), there are only two control parameters (k_1 and k_2) which S surface controller need to adjust. It is important to note that S surface controller can not get the best matching, whether adopting manual adjustment or adaptive adjustment. This is because that the adjustment is global and local adjustment is not available. Therefore, parameter adjustment is just the approximation of the system. After all, due to the complexity and uncertainty of control object, any kind of approach has big approximation. Thus, the optimal parameters k_1 and k_2 are different due to different velocities.

Manual adjustment of control parameters can make the motion control of underwater vehicle meet the demand in most cases. Response is more sensitive to small deviation but vibrations easily occur when k_1 and k_2 are larger. Therefore, the initial values of k_1 and k_2 we choose are generally about 3.0. If the overshoot is large, we can reduce k_1 and increase k_2 simultaneously. By contrast, if the speed of convergence is slow, we can increase k_1 and reduce k_2 simultaneously.

The ocean current and unknown disturbances can be considered as fixed disturbance force in a samlping period. Thus, we can eliminate the fixed deviation by adjusting the excursion of S surface and the function of control model is

$$u = 2.0/\left(1.0 + e^{(-k_1 e - k_2 \dot{e})}\right) - 1.0 + \Delta u \tag{34}$$

where Δu is the value(normalized) of fixed disturbance force which is obtained through adaptive manner. The adaptive manner is as follows:

a. Check whether the velocity of the vehicle is smaller than a preset threshold. If it is, go to step b), if not, go to step c);
b. Give the deviation value of this degree to a set array, at the same time, add 1 to the set counter, when the very counter reaches the predefined value, go to step d);
c. Shift each element in the array to the left by one, and at the meantime, decrease the counter by 1, then go to step a);
d. Weighted average the values of the array and the gained average deviation values are obtained. Then these deviation values are used to compute the side-play amount of control output, self-adapt the control output to eliminate fixed deviation, meanwhile, set the counter to zero, turn to the next loop.

Thus, a simple and practical controller is constructed, which can meet the work requirement in complicated ocean environment. However, the parameter adjustment of S surface controller is completely by hand. We hope to adjust the parameters for the controller by itself online, so we will present the self-learning algorithm the idea borrowed from BP algorithm in neural networks.

3.2 Self-learning algorithm

Generally, we define a suitable error function using neural networks for reference, so we can adjust the control parameters by BP algorithm on-line. As is known, an AUV has its own motion will, which is very important for self-learning and will be discussed in detail in the next section, so there is also an expected motion state. Namely, there is an expected control output for S surface controller. Therefore, the error function is given by

$$E_p = \frac{1}{2}(u_d - u)^2 \tag{35}$$

where u_d is the expected control output, and u is the last time output which can be obtained by eqution (34) .

We can use gradient descent optimization method, i.e. use the gradient of E_p to adjust k_1 and k_2.

$$\Delta k_i = -\eta \frac{\partial E_p}{\partial k_i} \tag{36}$$

where η is the learning ratio ($0 < \eta < 1$).

$$\frac{\partial E_p}{\partial k_i} = -(u_d - u) \cdot \frac{\partial u}{\partial k_i} = -(u_d - u) \cdot \frac{2.0 e^{-k_1 e - k_2 \dot{e}}}{(1 + e^{-k_1 e - k_2 \dot{e}})^2} e_i \tag{37}$$

where $i = 1,2$; $e_1 = e$; $e_2 = \dot{e}$

Therefore, k_1 and k_2 can be optimized by the following eqution.

$$k_i(t+1) = k_i(t) + \Delta k_i = k_i(t) + \eta(u_d - u) \cdot \frac{2 e^{-k_1 e - k_2 \dot{e}}}{(1 + e^{-k_1 e - k_2 \dot{e}})^2} \cdot e_i \tag{38}$$

We can get the expected speed by expected state programming. The expected control output can be obtained by the following principles.

If the speed v is less than or equal to v_d, then u is less than u_d, and u needs to be magnified. In the contrast, u needs to be reduced. The expected control output is given by

$$u_d = u + c \cdot (v_d - v) \tag{39}$$

where c is a proper positive constant. Therefore, S surface controller has the ability of self-learning.

3.3 AUV motion will

As an intelligent system, the AUV has motion will to some degree. It knows the expected speed and when and how to run and stop. The effect from environment changing is secondary, and it can overcome the distubance by itself. Certainly, the obility to overcome the distubance is not given by researchers, because they may not have the detailed knowledge of the changing of environment. Howerver, the AUV motion will can be given easily, because the artificial machine must reflect the human ideas. For example, when an AUV runs from the current state to the objective state, how to get the expected acceleration(motion will) can be considered synthetically by the power of thrusters, the working requirement and the energy consumption. However, the active compensation to various acting force (the reflective intelligence for achieving the motion will) will be obtained from self-learning. This is the path which we should follow for the AUV motion control (Peng, 1995).

The purpose of motion control is to drive the error **S** and the error variance ratio **V** between the current state and and the objective state to be zero. The pre-programming of control output is given by

$$\mathbf{a} = \mathbf{V} = \{a_x, a_y, a_z, a_\psi, a_\theta\} = f(\mathbf{S}, \mathbf{V}) \tag{40}$$

where the concrete form of $f(\cdot)$ can be given by synthetically consideration according to the drive ability of the power system.

$$\mathbf{a} = \mathbf{P}\mathbf{a}_{\max} \tag{41}$$

where $\mathbf{a}_{\max}$ is the AUV maximal acceleration, which lies on the drive ability of power system and the vehicle mass. $\mathbf{P}$ is given by

$$\mathbf{P} = \begin{bmatrix} p_1 & & & & 0 \\ & p_2 & & & \\ & & p_3 & & \\ & & & p_4 & \\ 0 & & & & p_5 \end{bmatrix} \tag{42}$$

where

$$\begin{cases} p_1 = (p_x / p_{xy}) \tanh(p_{xy} / 2) \\ p_2 = (p_y / p_{xy}) \tanh(p_{xy} / 2) \\ p_3 = \tanh(p_z / 2) \\ p_4 = \tanh(p_\psi / 2) \\ p_5 = \tanh(p_\theta / 2) \end{cases} \tag{43}$$

$$\begin{cases} p_x = S_x^* - c_x V_x \\ p_y = S_y^* - c_y V_y \\ p_z = S_z^* - c_z V_z \\ p_\psi = S_\psi^* - c_\psi V_\psi \\ p_\theta = S_\theta^* - c_\theta V_\theta \\ p_{xy} = \sqrt{p_x^2 + p_y^2} \end{cases} \tag{44}$$

where S_x^*, S_y^*, S_z^*, S_ψ^*, S_θ^* are difined as the traction distances in x, y, z, ψ, θ direction given by

$$S_i^* = \begin{cases} S_{i\max}^* & (S_i \geq S_{i\max}^*) \\ S_i & (-S_{i\max}^* < S_i < -S_{i\max}^*) \\ -S_{i\max}^* & (S_i \leq -S_{i\max}^*) \end{cases} \tag{45}$$

where $i = x$, y, z, ψ, θ. $S_{i\max}^*$ and c_i are undetermined coefficients, and $S_{i\max}^*$ are the predefined maximal distances which are determined based on the AUV's ability. We hope that the maximal transfer speed $V_{i\max}$

$$S_{i\max}^* - c_i V_{i\max} = 0 \tag{46}$$

As can be seen, we can not determine $S_{i\max}^*$ and c_i by equation (46), so we define the other constraint equation shown in equation (47).

$$\begin{cases} S_i'' = a_{i\max}\left(1 - \dfrac{2}{1+\exp\left(c_i S_i' - S_i\right)}\right), & (t > t_0) \\ S_i = S_{i\max}^* \\ S_i' = V_{i\max}, & (\mathrm{t} = \mathrm{t}_0) \end{cases} \tag{47}$$

Therefore, to all $t > t_0$, $S_i > 0$, and get smallest possible $t_n > t_0$. To all $t > t_n$, we can obtain

$$S_i < \varepsilon_i \tag{48}$$

where ε_i is the state precision. The constraint condition is to reduce errors as well as drive overshoot to zero.

4. Experiments

In this part, simulation and lake experiments have been conducted on WEILONG mini-AUV for many times to verify the feasibility and superiority of the mathmetical modelling and control method. The position errors of longitudinal control simulation are shown in Fig. 8. Reference inputs are 5m, the velocity of current is 0 m/s, and the voltage of thrusters is restricted by 2.5V. As can be seen, S surface control is feasible for the AUV motion control.
For the figure on the left, $k_1 = 8.0$ and $k_2 = 5.0$. Since the initial parameters are too big, there is certain overshoot and concussion aroud the object state in S surface control. However, the

parameters are adjusted by self-learning in improved S surface control. The overshoot is reduced and the balance (? Do you mean steady state) is achieved rapidly. For the figure on the right, $k_1 = 3.0$ and $k_2 = 5.0$. The initial parameters are too small, so the rate of convergence is too slow in S surface control. In improved S surface control, the rate of convergence is picked up and the performance is improved greatly.

Field experiments are conducted in the lake. The experiments use the impoved S surface control and the results are shown in Fig. 9 and Fig. 10. As there exits various disturbance (such as wave and current), the result curves are not smooth enough. In yaw control experiment, the action of the disturbances is greater than the acting force, so we can see some concussions in Fig. 9. It needs to be explained in the depth control that there is no response at the beginning of the experiment. The reason is the velocity of WEILONG mini-AUV is very low and the fin effect is too small. In the computer simulation, we don't use the fins until the velocity reaches certain value.

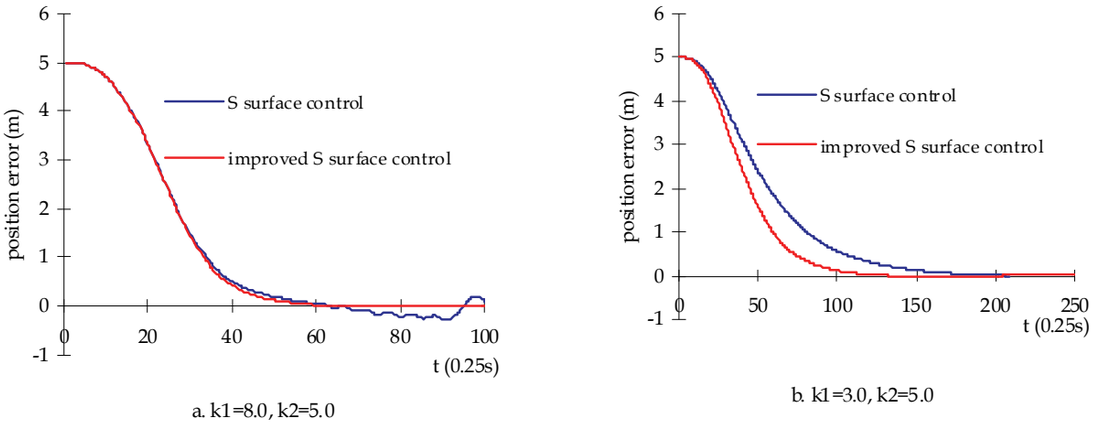

Fig. 8. Simulation results of longitudinal control

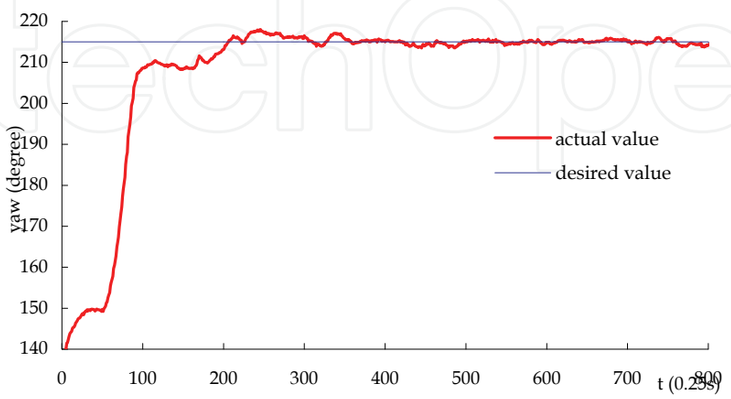

Fig. 9. Results of yaw control in lake experiments

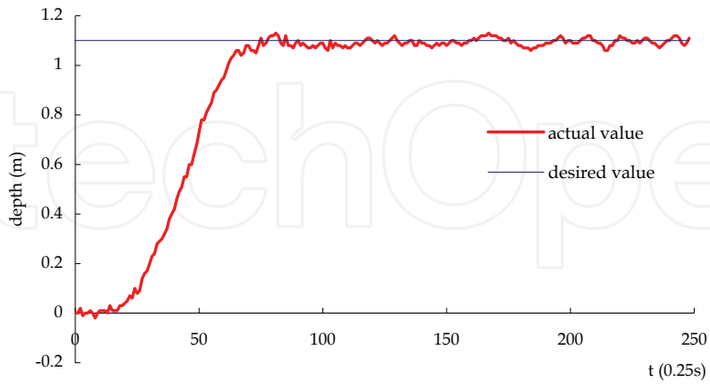

Fig. 10. Results of depth control in lake experiments

As can be seen, the control performance meets the requirement for the AUV motion control by using improved S surface control. It has high response speed and good robustness to various disturbances in field experiments.

5. Conclusion

This chapter concentrates on the problem of modeling and motion control for the AUVs with fins. Firstly, we develop the motion equation in six-degree freedom and analyze the force and hydrodynamic coefficients, especilly the fin effect. The feasibility and accuracy are verified by comparing the results between at-sea experiments and simulation. The model is applicable to most AUVs. Secondly, we present a simple and practical control method—S surface control to achieve motion control for the AUVs with fins, and deduce the self-learning algorithm using BP algorithm of neural networks for reference. Finally, the experiment results verify the feasibility and the superiority of the mathmetical modelling and control method.

6. Acknowledgements

The authors wish to thank all the researchers at the AUV Lab in Harbin Engineering University without whom it would have been impossible to write this chapter. Specifically, the authors would like to thank Professor Yuru Xu who is the subject leader of Naval Architecture and Ocean Engineering in Harbin Engineering University and has been elected as the member of Chinese Academy of Engineering since 2003. Moreover, the authors would like to thank Pang Shuo who is an assistant professor of Embry-Riddle Aeronautical University in USA.

7. References

Blidberg D.R. (1991). Autonomous underwater vehicles: a tool for the ocean, *Unmanned Systems*, Vol. 9, No. 2, 10-15, 1991.

Xu Y.R.; Pang Y.J.; Gan Y. & Sun Y.S. (2006). AUV-state-of-the-art and prospect. *CAAI Transactions on Intelligent Systems*, Vol.1, No.1, 9-16, September 2006.

Xu Y.R. & Xiao K. (2007). Technology development of autonomous ocean vehicle. *Journal of Automation*, Vol. 33, No. 5, 518-521, 2007.

Conte G. & Serrani A. (1996). Modelling and simulation of underwater vehicles. *Proceedings of the 1996 IEEE International Symposium on Computer-Aided Control System Design*, pp. 62-67, Dearborn, Michigan, September 1996

Timothy P. (2001). Development of a Six-Degree of Freedom Simulation Model for the REMUS Autonomous Underwater Vehicle: Oceans. *MTS/IEEE Conference and Exhibition*, pp. 450-455, May 2001

Prestero T. J. (2001). Development of a six-degree of freedom simulation model for the remus autonomous underwater vehicle. *Proceedings of the OCEANS 2001 MTS/IEEE Conference and Exhibition*, pp. 450-455, Honolulu, Hawaii, November 2001

Ridley P.; Fontan J. & Corke P. (2003). Submarine dynamic modeling. *Proceedings of the Australian Conference on Robotics and Automation*, Brisbane, Australia, December 2003

Chang W.J.; Liu J.C. & Yu H.N. (2002). Mathematic model of the AUV motion control and simulator. *Ship Engineering*, *y*, Vol.12, No.3, 58-60, September 2002.

Li Y.; Liu J.C. & Shen M.X.(2005). Dynamics model of underwater robot motion control in 6 degrees of freedom. *Journal of Harbin Institute of Technology*, Vol.12, No.4, 456-459, December 2005.

Nahon M. (2006). A Simplified Dynamics Model for Autonomous Underwater Vehicles. *Journal of Ocean Technology*, Vol. 1, No. 1, pp. 57-68, 2006

Silva J.; Terra B.; Martins R. & Sousa J. (2007). Modeling and Simulation of the LAUV Autonomous Underwater Vehicle. *Proceedings of the 13th IEEE IFAC International Conference on Methods and Models in Automation and Robotics*, pp. 713-718, Szczecin, Poland, August 2007

Su Y.M.; Wan L. & Li Y. (2007). Development of a small autonomous underwater vehicle controlled by thrusters and fins. *Robot*, Vol. 29, No. 2, 151-154, 2007.

Shi S.D. (1995). *Submarine Maneuverability*. National Defence Industry Press, Beijing.

Louis A.G. (2004). Design, modelling and control of an autonomous underwater vehicle. *Bachelor of engineering honours thesis*, University of Western Australia, 2004.

Giuseppe C. (1999). Robust Nonlinear Motion Control for AUVs. *IEEE Robotics & Automation Magazine*. pp. 33-38, May 1999

Peng L.; Lu Y.C. & Wan L. (1995). Neural network control of autonomous underwater vehicles. *Ocean Engineering*, Vol.12, No.2, 38-46, December 1995.

Liu X.M. & Xu Y.R. (2001). S control of automatic underwater vehicles. *Ocean Engineering*, Vol.19, No.3, 81-84, September 2001.

Liu J.C.; Yu H.N. & Xu Y.R. (2002). Improved S surface control algorithm for underwater vehicles. *Journal of Harbin Engineering University*, Vol.23, No.1, 33-36, March 2002.

Underwater Vehicles

Edited by Alexander V. Inzartsev

ISBN 978-953-7619-49-7

Hard cover, 582 pages

Publisher InTech

Published online 01, January, 2009

Published in print edition January, 2009

For the latest twenty to thirty years, a significant number of AUVs has been created for the solving of wide spectrum of scientific and applied tasks of ocean development and research. For the short time period the AUVs have shown the efficiency at performance of complex search and inspection works and opened a number of new important applications. Initially the information about AUVs had mainly review-advertising character but now more attention is paid to practical achievements, problems and systems technologies. AUVs are losing their prototype status and have become a fully operational, reliable and effective tool and modern multi-purpose AUVs represent the new class of underwater robotic objects with inherent tasks and practical applications, particular features of technology, systems structure and functional properties.

InTech Europe

University Campus STeP Ri
Slavka Krautzeka 83/A
51000 Rijeka, Croatia
Phone: +385 (51) 770 447
Fax: +385 (51) 686 166
www.intechopen.com

InTech China

Unit 405, Office Block, Hotel Equatorial Shanghai
No.65, Yan An Road (West), Shanghai, 200040, China
中国上海市延安西路65号上海国际贵都大饭店办公楼405单元
Phone: +86-21-62489820
Fax: +86-21-62489821

IntechOpen